Mathematisches Forschungsinstitut Oberwolfach

Report No. 37/2020

DOI: 10.4171/OWR/2020/37

Mini-Workshop: Nonlocal Analysis and the Geometry of Embeddings (hybrid meeting)

Organized by
Simon Blatt, Salzburg
Philipp Reiter, Chemnitz
Armin Schikorra, Pittsburgh

22 November – 28 November 2020

Abstract. Both self-avoidance and self-contact of geometric objects can be modeled using repulsive energies that separate isotopy classes. Giving rise to nonlocal operators, they are interesting objects in their own right. Moreover, their analytical structure allows for devising numerical schemes enjoying robust features such as energy stability. This workshop aimed at discussing recent trends in this matter, including potential applications to modeling.

Mathematics Subject Classification (2010): 53C 58C 65M 70E.

Introduction by the Organizers

The study of self-contact preventing energies started roughly thirty years ago with the definition of so-called knot energies. The underlying concepts trace back to earlier work by Menger in the 1930s and Federer in the 1950s.

In pursuit of finding nicely shaped representatives within isotopy classes, a variety of different functionals such as ropelength and its smooth variants has been proposed. This stimulated quite a lot of activity in both geometric topology and geometric analysis. These efforts were partly motivated by the idea to pave a new way to the decision problem in knot theory.

While preventing self-contact and thereby self-penetrations, the functionals provide a "measure" for the quality of an embedding. Subsequently, interesting connections to harmonic analysis surfaced. By their nature, repulsive energies are

highly nonlocal. Many of them naturally lead to fractional Sobolev spaces, providing yet another motivation for investigating these.

The respective Euler–Lagrange equations and the corresponding evolution equations are nonlocal geometric PDEs whose analysis turns out to be particularly challenging. Furthermore, the design of efficient optimization schemes demands a deep understanding of the structure of the underlying operators.

The concept of repulsive energies is also related to fundamental questions in topology. It is still unclear whether there is a gradient flow of some knot energy that realizes a retract of the trivial loops to round circles. Although such a mechanism exists due to the Smale conjecture, no explicit construction is known so far. Of course, any candidate functional must not admit critical points within the unknot class apart from circles.

Even more importantly for applications, repulsive energies can also be employed to model steric constraints. This is normally achieved via a regularization approach that is both analytically and numerically demanding. In particular, it involves fine-tuning of several parameters. For instance, in the case of the elastic energy, strong forces related to bending effects have to be compensated by repulsive forces related to the regularization term in order to avoid self-intersections. However, analytical properties of the energy may allow for proving rigorous results on discrete flows which are not feasible for some ad-hoc approaches that are employed in applications.

Qualitative properties of minimizers often rely on intricate topological results. For instance they can be used in order to extend lower bounds on energies in given isotopy classes to larger domains. Moreover, the topology of the respective energy landscape seems to be quite complex. In some cases it remains an open question whether minimizers or stationary points within certain isotopy classes exist at all.

Overall, this field seems to be particularly appealing due to the synthesis of questions and tools at the interface of topology, analysis, numerics, optimization, and modeling.

The mini-workshop *Nonlocal Analysis and the Geometry of Embeddings*, organised by Simon Blatt (Salzburg), Philipp Reiter (Chemnitz), and Armin Schikorra (Pittsburgh), took place under the restrictions imposed by the covid-19 pandemic. However, this situation provided the opportunity to implement an actual "workshop" format that focused on discussions, mostly in plenum, rather than talks.

The workshop gathered researchers from different fields such as topology, geometric and harmonic analysis, numerics, and elasticity theory. Particular attention was paid to including early career researchers, a third of our participants being doctoral students.

In order to enable everyone to participate, a hybrid format has been implemented. Thereby eleven participants from Austria, the Czech Republic, Germany, Poland, Switzerland, and the United States have been included remotely. A number of seven people residing in Germany could actually stay in person at Oberwolfach.

The technical facilities allowed for bridging the gap between these two groups. The amount of interaction exceeded the expectations by far, resulting in a lot of intense discussions. Unfortunately, due to different time zones the US participants were to miss the morning sessions. However, in order not to discourage anyone from sharing ideas and conjectures, the discussions have not been recorded.

On Monday and Tuesday afternoon two sessions of five short talks each were held. In particular, young participants were given the opportunity to present a current research project at this occasion. Furthermore, a couple of additional talks were included in the course of the workshop. By special agreement with the institute, the talk by John Maddocks on Tuesday evening was streamed as a part of a weekly hosted online seminar run by the same group of organizers.

At the first day, a preliminary schedule for the rest of the week was set by identifying questions of common interest. Topics that were discussed extensively include regularity issues and gradient flows, numerics, applications in elasticity theory, namely elastic rod theories, and the energy landscape within isotopy classes, mainly focusing on critical points within the unknot class.

While curves with and without frames constitute the central class of examples, the workshop clearly demonstrated the availability of both theoretical and computational tools being required for the treatment of surfaces. One may expect some progress in this direction in near future. A couple of new energy functionals have been proposed that may be better suited in the context of higher-dimensional objects.

The concept sketched above seems to have worked out. For instance, this is demonstrated by the fact that one strand of the discussion has been continued via email between many workshop participants for about two weeks after the meeting.

Despite the difficult circumstances, the participants experienced a true Oberwolfach atmosphere which did not only consist of intense scientific interaction but also comprised social activities such as the traditional hiking tour which has been shifted to Thursday morning.

Overall, direction and staff of the MFO did great efforts to accommodate both online and on-site participants which highly added to the success of this workshop.

Mini-Workshop (hybrid meeting): Nonlocal Analysis and the Geometry of Embeddings

Table of Contents

Abstracts

Möbius-invariant self-avoidance energies for non-smooth sets in arbitrary dimensions

Heiko von der Mosel
(joint work with Bastian Käfer)

The Möbius-invariance of J. O'Hara's well-known Möbius energy [7] for closed curves $\gamma : \mathbb{R}/\mathbb{Z} \to \mathbb{R}^n$ can easily be seen using Doyle and Schramm's *cosine formula*

$$E_{\text{Möb}}(\gamma) = \int_\gamma \int_\gamma \frac{1-\cos\vartheta_\gamma(x,y)}{|x-y|^2}\, d\mathscr{H}^1(x) d\mathscr{H}^1(y), \tag{1}$$

where $\vartheta_\gamma(x,y)$ denotes the *conformal angle* between the two circles $\mathbb{S}^1(x,x,y)$ and $\mathbb{S}^1(y,y,x)$ through x and y, the first circle being tangent to the curve γ at x, and the second tangent to γ at y; see [8, Chapter 3.4]. Indeed, the numerator of the energy density depends only on the angle which by definition is invariant under any conformal transformation, and this numerator is integrated against the conformally-invariant singular measure $|x-y|^{-2}\, d\mathscr{H}^1(x)\mathscr{H}^1(y)$. R. B. Kusner and J. M. Sullivan pointed out in [6] that the same is true in higher dimensions: Integrating a purely angle-dependent function $L(\vartheta_{\mathscr{M}}(x,y))$ such as $(1-\cos\vartheta_{\mathscr{M}}(x,y))^m$ against the singular surface measure $|x-y|^{-2m}\, d\mathscr{H}^m(x) d\mathscr{H}^m(y)$ over the cartesian product $\mathscr{M} \times \mathscr{M}$ of an embedded C^1-submanifold $\mathscr{M} \subset \mathbb{R}^n$ gives rise to Möbius-invariant energy functionals. Here, $\vartheta_{\mathscr{M}}(x,y)$ is the conformal angle between the two unique m-dimensional tangential spheres $\mathbb{S}^m(x,x,y)$ tangent to $\mathscr{M}$ at x, and $\mathbb{S}^m(y,y,x)$ tangent to $\mathscr{M}$ at y and both containing both points x and y.

Motivated by variational considerations we extend in [2, 3] the domain of such energy functionals to a wide class of non-smooth admissible sets $\Sigma \subset \mathbb{R}^n$, prove self-avoidance effects of the energies, and show that every embedded submanifold of a mild fractional Sobolev regularity has finite energy. The class of admissible sets Σ contains in particular finite unions of immersed compact C^1-manifolds or embedded compact Lipschitz submanifolds, as well as countably infinite unions of entire Lipschitz graphs, but also sets (possibly of full n-dimensional measure) that can be foliated by m-dimensional submanifolds of uniformly bounded curvature; see Figure 1.

To formulate the precise statements let $\mathscr{G}(n,m)$ denote the Grassmannian of all m-dimensional subsets of $\mathbb{R}^n$, equipped with the angle metric $\measuredangle(F,G) := \|\Pi_F - \Pi_G\|$ for $F, G \in \mathscr{G}(n,m)$, where Π_F, Π_G denote the orthogonal projections onto F and G, respectively. Moreover, we denote by $C_x(\beta, F) := \big\{ z \in \mathbb{R}^n : \big|\Pi_{F^\perp}(z-x)\big| \leq \beta \big|\Pi_F(z-x)\big| \big\}$ the cone around the affine m-plane $x+F$, centered at the point $x \in \mathbb{R}^n$ with opening angle $2\arctan\beta$.

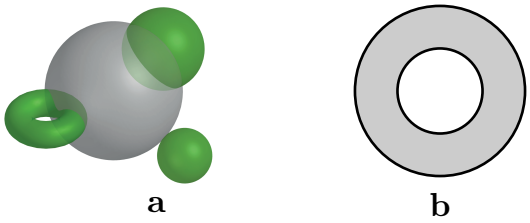

FIGURE 1. **Admissible sets.** Finite unions of smooth submanifolds (**a**) and the annulus (**b**) as the uncountable union of circles with positively bounded radii are contained in $\mathscr{A}^m(\alpha, M)$ for all $\alpha, M > 0$.

Definition 1 (Admissible sets)**.** [1] Let $m, n \in \mathbb{N}$, $1 \leq m \leq n$, $\alpha > 0$, $M > 0$. Then the *admissibility class* $\mathscr{A}^m(\alpha, M)$ is the set of all closed subsets $\Sigma \subset \mathbb{R}^n$ equipped with a function $H\colon \Sigma \to \mathscr{G}(n, m)$ satisfying the following: There exists a dense subset $\Sigma^* \subset \Sigma$ such that for all compact sets $K \subset \Sigma$, there are a radius $R_K > 0$ and a constant $c_K > 0$, such that for all $p \in \Sigma^* \cap K$, there is a dense subset $D_p \subset (p + H(p)) \cap B_{R_K}(p)$, such that for all $x \in D_p$, there exists a point $\eta_x \in \Sigma \cap C_p(\alpha, H(p))$ with $\Pi_{p+H(p)}(\eta_x) = x$, and

$$\mathscr{H}^m\left(E_{\alpha,M}(p) \cap B_r(\eta_x)\right) \geq c_K r^m \text{ for all } r \in \left(0, R_K/10^5\right],$$

where $E_{\alpha,M}(p) := \{\mu \in \Sigma : \ \sphericalangle(H(\mu), H(p)) < M\alpha\}$.

Now we define a one-parameter family of Möbius-invariant energies. For given $\tau \in \mathbb{R}$, $\alpha, M > 0$, and $\Sigma \in \mathscr{A}^m(\alpha, M)$ set

$$E^\tau(\Sigma) := \int_\Sigma \int_\Sigma \frac{\sphericalangle\left(\mathbb{S}^m(x,x,y), \mathbb{S}^m(y,y,x)\right)^{(1+\tau)m}}{|x-y|^{2m}}\, d\mathscr{H}^m(x) d\mathscr{H}^m(y), \tag{2}$$

where now the classic tangent planes at x and y are replaced by the "mock" tangent planes $H(x)$ and $H(y)$, to determine the conformal angle between the tangential spheres $\mathbb{S}^m(x,x,y)$ and $\mathbb{S}^m(y,y,x)$ as the angle between $H(x)$ and the reflection[2] of $H(y)$ at the hyperplane $(x-y)^\perp$. We say that an admissible (and therefore possibly non-compact) set Σ *has locally finite energy* if $E^\tau(\Sigma \cap B_N(0)) < \infty$ for all $N \in \mathbb{N}$. Notice that we work with the angle metric to measure the angle in contrast to Kusner and Sullivan who use the principal angles $0 \leq \vartheta_1 \leq \cdots \leq \vartheta_m \leq \pi/2$ to form the *combined* angle ϑ by means of $\cos\vartheta := \Pi_{i=1}^m \cos\vartheta_i$. But we can relate our energies E^τ to their cosine energy: for $\tau \in [0, 1)$ our energy dominates theirs, whereas for $\tau \in (1, \infty)$ their energy dominates E^τ up to a multiplicative constant.

[1] This class is not directly comparable to the admissibility classes considered in previous work on geometric curvature energies on non-smooth sets. The requirement of a *uniform* R_K for a given compact set $K \subset \Sigma$ is stronger, whereas we presently do not require that Σ is locally *contained* in a cone as in [10], nor do we assume any relation between the Jones' β- and Reifenberg's θ-numbers as, e.g., in [5].

[2] This convenient way to compute this angle was already pointed out by Kusner and Sullivan [6, Section 11].

For $\tau = 1$, however, E^τ is equivalent to the cosine energy of Kusner and Sullivan, so that any of the following results specified to the case $\tau = 1$ holds for their cosine energy as well.

Theorem 1 (Self-avoidance)**.** *For fixed dimensions $2 \leq m \leq n$ there is a universal constant $\delta = \delta(m)$ such that for any $\alpha, M > 0$ with*

$$\alpha(M+1) < \delta/50 \tag{3}$$

every admissible set $\Sigma \in \mathscr{A}^m(\alpha, M)$ with locally finite Möbius energy E^τ, $\tau \in (-1, \infty)$, is an embedded Lipschitz submanifold of $\mathbb{R}^n$.

Initially granted smoothness of an admissible set transfers to the submanifolds obtained by finite energy.

Corollary 1. *Let $k \in \mathbb{N}$ and suppose $\Sigma = f(\mathscr{M})$ satisfies $E^\tau(\Sigma) < \infty$ for $\tau \in (-1, \infty)$, where $\mathscr{M}$ is an m-dimensional compact C^k-manifold, and $f : \mathscr{M} \to \mathbb{R}^n$ is a C^k-immersion. Then Σ is an embedded m-dimensional C^k-submanifold of $\mathbb{R}^n$.*

The equivalence of the Kusner-Sullivan cosine energy with E^τ for $\tau = 1$ together with Corollary 1 might help to generalize O'Hara's recent C^2-self-repulsiveness result [9, Theorem 3.3] to suitably normalized C^1-submanifolds in the C^1-topology.

In view of Theorem 1 and Corollary 1 one may ask, on the other hand, what regularity of embedded submanifolds actually guarantees finite energy. It turns out that a relatively low fractional Sobolev regularity suffices.

Theorem 2 (Sufficient fractional Sobolev regularity)**.**
If $\mathscr{M}^m \subset \mathbb{R}^n$ is an embedded compact submanifold with local graph representations of class $C^{0,1} \cap W^{\frac{2+\tau}{1+\tau},(1+\tau)m}$ for some $\tau \in (0, \infty)$, then $E^\tau(\mathscr{M}) < \infty$.

This shows in particular for $\tau = 1$ that embedded submanifolds with local graph representations of class $C^{0,1} \cap W^{3/2,2m}$ have finite E^τ-energy, and hence also finite cosine energy. Open at this point, however, is if finite energy implies exactly that fractional Sobolev regularity[3]. Such an energy space characterization is what one would hope for in view of S. Blatt's result for $m = 1$ [1, Theorem 1.1]. We know that our energies E^τ do exhibit regularizing effects: by direct computation one can show that a wedge-type singularity produces an infinite amount of energy, so finite energy implies a regularity beyond Lipschitz. Since our estimates for Theorem 1 depend on the absolute continuity of the energy's integral we do not have a priori estimates on the size of local graph patches depending only on the energy value. This would be very helpful for variational applications such as energy minimization in prescribed isotopy classes.

[3]For the scale-invariant tangent-point energy such a characterization for C^1-submanifolds holds true; see [4].

References

[1] S. Blatt, *Boundedness and regularizing effects of O'Hara's knot energies*, Journal of Knot Theory and Its Ramifications **1** (2012), 1250010, 9.

[2] B. Käfer, *Scale-invariant geometric curvature functionals, and characterization of Lipschitz- and C^1-submanifolds*, PhD thesis, RWTH Aachen University, 2020, under review.

[3] B. Käfer and H. von der Mosel, *Möbius-invariant self-avoidance energies for non-smooth sets in arbitrary dimensions*, arXiv e-prints (Oct. 2020), arXiv:2010.03906.

[4] B. Käfer and H. von der Mosel, *On scale-invariant tangent-point energies in arbitrary dimensions*, (2021), in preparation.

[5] S. Kolasiński, P. Strzelecki, and H. von der Mosel, *Characterizing $W^{2,p}$ submanifolds by p-integrability of global curvatures.* Geometric and Functional Analysis **23**(3) (2013), 937–984.

[6] R. B. Kusner and J. M. Sullivan, *Möbius energies for knots and links, surfaces and submanifolds.* In: *Geometric topology (Athens, GA, 1993)*, AMS/IP Studies in Advanced Mathematics, vol. 2, American Mathematics Society, Providence, RI, 1997, 570–604.

[7] J. O'Hara, *Energy of a knot*, Topology **30**(2) (1991), 241–247.

[8] J. O'Hara, *Energy of knots and conformal geometry*, Series on Knots and Everything, vol. 33, World Scientific Publishing Co. Inc., River Edge, NJ (2003).

[9] J. O'Hara, *Self-repulsiveness of energies for closed submanifolds*, arXiv e-prints (Apr. 2020), arXiv:2004.02351.

[10] P. Strzelecki, and H. von der Mosel, *Tangent-point repulsive potentials for a class of non-smooth m-dimensional sets in $\mathbb{R}^n$. Part I: Smoothing and self-avoidance effects*, Journal of Geometric Analysis **23**(3) (2013), 1085–1139.

Variational approach to the Arnold invariants of immersed planar curves via knot energies

Anna Lagemann

The talk is based on the current research results of my dissertation. Planar immersed curves can be classified by the Whitney-Graustein theorem up to regular homotopy, which states that the space of immersions of the circle into the plane with the same winding number of the tangent-vector is connected. In other words, the winding number is an invariant in the space of immersions. Arnold took a much deeper look into so-called generic immersions, these are curves where all self-intersection points are transverse double points [1]. The set of all non-generic immersions is called the discriminant. Arnold then defined three important parts of the discriminant that correspond to a certain type of non-generic immersions: curves with direct and inverse self-tangencies and curves with triple points. His idea was to define three invariants J^+, J^- and St that are dual to these three parts of the discriminant. It turns out that the discriminant is indeed a hypersurface in the space of immersions with codimension one and the three parts mentioned above are co-oriented. Due to the Whitney-Graustein theorem one can find a homotopy in the space of immersions between any two immersions with the same winding number. Furthermore, that homotopy can be chosen in such a way that it intersects the discriminant only in the above mentioned three parts in a transverse manner. The co-orientation of the discriminant then delivers a sign at those intersections. Now the three invariants are defined as follows: For each winding number a representative curve will be fixed and on those curves the values of the

invariants are prescribed. Then one establishes precise rules on how the invariants change along a homotopy in the space of immersions at intersections with the discriminant according to the signs at the intersections. Arnold proved that those invariants exist and are uniquely defined by the normalizing conditions on the representative curves. The question that arises is to what extent a connected component in the complement of the discriminant - i.e. generic immersions with prescribed values of J^+, J^- and St - is a "potential well" for some knot energy.

In general, knot energies have infinite values on curves that exhibit self-intersections. But planar curves without self-intersections are embedded and therefore homotopic to the circle. Therefore, we will consider an energy that is truncated near the points of self-intersection, an approach that Dunning used in his dissertation [2]. Since we are dealing with immersions it is natural to consider a knot energy that takes derivatives into account, a potentially suitable energy is the tangent-point energy introduced by Gonzalez and Maddocks [3] and investigated in detail by Strzelecki and von der Mosel [4] and Blatt [5].

Definition 1. Let $\gamma \in C^1\left(\mathbb{R}/\mathbb{Z}, \mathbb{R}^2\right)$ be a rectifiable curve of unit length and be parametrized by arclength. For any $2 \leq q < \infty$ we define the tangent-point energy

$$\mathcal{E}^q(\gamma) := \iint\limits_{(\mathbb{R}/\mathbb{Z})^2} \left(\frac{2\,\mathrm{dist}(l(t), \gamma(s))}{|\gamma(t) - \gamma(s)|^2}\right)^q dsdt,$$

where $l(t) := \{\gamma(t) + \lambda\gamma'(t) \mid \lambda \in \mathbb{R}\}$ is the tangent line at the point $\gamma(t)$.

As a first step, we look at the simple case of figure-eight shaped cuves, denote by I_1 be the isotopy class of planar figure-eight shaped curves.

Definition 2. Let $\lambda \in \left(0, \frac{1}{2}\right]$ and $\eta \in \left[0, \frac{\lambda}{4}\right)$. Define $F_{\lambda,\eta} \subset I_1 \cap C^1\left(\mathbb{R}/\mathbb{Z}, \mathbb{R}^2\right)$ as the subset of all curves $\gamma \in I_1 \cap C^1\left(\mathbb{R}/\mathbb{Z}, \mathbb{R}^2\right)$ satisfying

(1) The curve γ has unit length.
(2) The curve γ is parametrized by arclength.
(3) The self-intersection is at the origin.
(4) The self-intersection is transversal.
(5) Within arclength η of the self-intersection, γ consists of two linear segments.
(6) If $u, v \in \mathbb{R}/\mathbb{Z}$ are the distinct times that yield the self-intersection, the length of the shorter arc $d_\gamma(\gamma(u), \gamma(v))$ equals λ.

Hence, curves in $F_{\lambda,\eta}$ look like a skewed plus-sign around the self-intersection. Then we define the troublesome set

$$\begin{aligned} Y_\delta := \big\{(x,y) \in (\mathbb{R}/\mathbb{Z})^2 \mid\ & (|x-u| < \delta \text{ and } |y-v| < \delta) \text{ or} \\ & (|x-v| < \delta \text{ and } |y-u| < \delta)\big\}. \end{aligned}$$

The δ-renormalized energy of $\gamma \in F_{\lambda,\eta}$ is then defined as

$$\mathcal{E}^q_\delta(\gamma) := \iint\limits_{(\mathbb{R}/\mathbb{Z})^2 \setminus Y_\delta} \left(\frac{2\,\mathrm{dist}(l(t), \gamma(s))}{|\gamma(t) - \gamma(s)|^2}\right)^q dsdt.$$

In the previously defined class of curves there exists a minimizer of the δ-renormalized tangent-point energy:

Theorem 1. *Let $q > 2$, $\lambda \in \left(0, \frac{1}{2}\right]$ and $\eta \in \left[0, \frac{\lambda}{5}\right)$. Then for every $\delta \in (0, \eta]$ there exists an immersion $\gamma_\delta^\eta \in F_{\lambda,\eta}$ such that*

$$\mathcal{E}_\delta^q\left(\gamma_\delta^\eta\right) \leq \mathcal{E}_\delta^q(\gamma) \text{ for all } \gamma \in F_{\lambda,\eta}.$$

A question that naturally arises is whether it is possible to send the truncation parameter δ to zero and obtain a converging subsequence of minimizers and investigate geometric properties of the limit curve. The following theorems are still work in progress.

Theorem 2. *Let $q > 2$, $\lambda \in \left(0, \frac{1}{2}\right]$ and $0 < \delta < \eta$ for η sufficiently small. Further, let $\gamma_\delta^\eta \in F_{\lambda,\eta}$ be a minimizer of $\mathcal{E}_\delta^q$. Then there exists a curve $\Gamma^\eta \in F_{\lambda,\eta}$ and a subsequence, again denoted by $(\gamma_\delta^\eta)_{\delta>0}$, such that*

$$\gamma_\delta^\eta \xrightarrow{C^1} \Gamma^\eta \quad \text{as } \delta \to 0.$$

Theorem 3. *The limit curve Γ^η intersects itself at a right angle.*

References

[1] V. Arnold, *Topological invariants of plane curves and caustics*, University Lecture Series, vol. 5, American Mathematical Society, Providence, RI, 1994. Dean Jacqueline B. Lewis Memorial Lectures presented at Rutgers University, New Brunswick, New Jersey.

[2] R. Dunning, *Asymptotics under Self-Intersection for Minimizers of Self-Avoiding Energies*, Phd Thesis, Rice University, 2009.

[3] O. Gonzalez, J. H. Maddocks, *Global curvature, thickness, and the ideal shape of knots*, Proceedings of the National Academy of Sciences of the United States of America **96**(9) (1999), 4769–4773.

[4] P. Strzelecki, H. von der Mosel, *Tangent-point self-avoidance energies for curves*, Journal of Knot Theory and Its Ramifcations, **21**(5), 1250044-1–1250044-28.

[5] S. Blatt, *The energy spaces of the tangent point energies*, Journal of Topology and Analysis **5**(3) (2013), 261–270.

A finite element approach for the computation of the Möbius energy

Lothar Banz

(joint work with Simon Blatt)

A widely discussed task is the computation of an energy minimizing knot. Most often the chosen energy is the so-called Möbius energy

$$E(\gamma) \coloneqq \int_0^1 \int_0^1 \left[\frac{1}{|\gamma(y) - \gamma(x)|^2} - \frac{1}{D(\gamma(y), \gamma(x))^2}\right] |\dot{\gamma}(y)||\dot{\gamma}(x)|\, dy\, dx$$

with $D(\gamma(y), \gamma(x)) = \min\left\{\int_{\min\{x,y\}}^{\max\{x,y\}} |\dot{\gamma}(t)|\, dt, L - \int_{\min\{x,y\}}^{\max\{x,y\}} |\dot{\gamma}(t)|\, dt\right\}$ for a non-intersecting, rectifiable curve $\gamma : [0,1] \to \mathbb{R}^3$ of length L. Crucial for the necessary

numerical scheme is the discretization of the otherwise infinite dimensional minimization problem. For that we may replace the knot γ by some finite element knot $\gamma_{hp} \in V_{hp}^{(s)}$ with the finite dimensional space

$$V_{hp}^{(s)} := \left\{ v_{hp} \in \left[C^s_{per}[0,1] \right]^3 : v_{hp}|_{I_i} \circ \mathcal{F}_i \in \left[\mathbb{P}_{p_i}[-1,1] \right]^3,\ 0 \le i \le n \right\}.$$

Here, n denotes the number of elements, each element has the length h_i, p_i is the local polynomial degree and

$$C^s_{per}[a,b] := \left\{ v \in C^s[a,b] : v^{(i)}(a) = v^{(i)}(b),\ 0 \le i \le s \right\}.$$

We discuss several challenges in the evaluation of $E(\gamma_{hp})$ such as the choice of quadrature formulas, singularities of the integrands and loss of significant error. We show that if γ_{hp} is the L^2-projection of some knot γ then there holds

$$\begin{aligned} E(\gamma) - E(\gamma_{hp}) = \frac{1}{2}(\gamma - \gamma_{hp}, z) + \frac{1}{2}(\nabla E(\gamma_{hp}) - z_{hp}, \gamma - v_{hp}) \\ + \frac{1}{2}\int_0^1 \nabla^3 E(\gamma_{hp} + se)(e,e,e) \cdot s(s-1)\, ds \end{aligned}$$

with $e = \gamma - \gamma_{hp}$, $z = \nabla E(\gamma)$ and

$$z_{hp} \in V_{hp}^{(s)} : \quad (z_{hp} - \nabla E(\gamma_{hp}), \psi_{hp}) = 0 \quad \forall \psi_{hp} \in V_{hp}^{(s)},$$

leading to an easy to implement, efficient and reliable a posteriori error estimate on the signed Möbius energy error. Crucial for its numerical efficiency is the alternative representation of the gradient

$$\begin{aligned} \nabla E(\gamma)(\varphi) = \int_I \int_I \Bigg\{ q\left(\frac{2\widetilde{D}(x,y)}{L}\right) \frac{1}{\widetilde{D}^2(x,y)} \left\langle \frac{\dot\gamma(y)}{|\dot\gamma(y)|} - \frac{\dot\gamma(x)}{|\dot\gamma(x)|}, \frac{\dot\varphi(y)}{|\dot\gamma(y)|} - \frac{\dot\varphi(x)}{|\dot\gamma(x)|} \right\rangle \\ - 2\langle \gamma(y) - \gamma(x), \varphi(y) - \varphi(x) \rangle \left[\frac{1}{|\gamma(y) - \gamma(x)|^4} - \frac{1}{\widetilde{D}^4(x,y)} \right] \\ + 2\frac{\langle \dot\gamma(x), \dot\varphi(x) \rangle}{|\dot\gamma(x)|^2} \left[\frac{1}{|\gamma(y) - \gamma(x)|^2} - \frac{1}{\widetilde{D}^2(x,y)} \right] \Bigg\} |\dot\gamma(y)||\dot\gamma(x)|\, dy\, dx \end{aligned}$$

with $q(t) = \frac{2}{3}t^3 - t^2 + \frac{1}{3}$ and $\widetilde{D}(x,y) = D(\gamma(y), \gamma(x))$.
We present several numerical examples showing that the error $E(\gamma) - E(\gamma_{hp})$ exhibits a convergences rate depending on p and s of at least 5 with respect to the dimension of $V_{hp}^{(s)}$ and may even be exponential if γ is sufficiently smooth. In all experiments the efficiency index (a posteriori error estimate divided by signed error) is, as typical for DWR ones, (almost) one.

Fractional Operators: Analysis, Control, and Applications

Harbir Antil

Fractional calculus and its application to anomalous diffusion has recently received a tremendous amount of attention. In complex/heterogeneous material mediums, the long-range correlations or hereditary material properties are presumed to be the cause of such anomalous behavior. Owing to the revival of fractional calculus, these effects are now conveniently modeled by fractional-order differential operators and the governing equations are reformulated accordingly. We begin this talk by discussing one such application of fractional Laplacian in geophysical electromagnetism [17]. Here, we have derived the fractional Helmholtz equation from first principle arguments in conjunction with a constitutive relationship.

Besides capturing nonlocality (long range effects), fractional Laplacian enforces less smoothness than its classical counterpart. As a result, it is excellent in capturing sharp transitions across interfaces. We illustrate the effect of using fractional Laplacian as a regularizer in image denoising problems. Recall that, typically one uses Total Variation (TV) seminorm as a regularizer in such settings [15]. We establish that one can obtain comparable results using fractional Laplacian and our proposed approach is significantly cheaper, one only needs to solve a linear equation instead of the nonlinear/degenerate problem in case of TV [1]. A bilevel optimization framework to identify the fractional exponent is provided in [5].

In a bounded domain $\Omega \subset \mathbb{R}^N$ with boundary $\partial\Omega$, there are several ways to define fractional Laplacian. We consider the two most popular ones. With fractional exponent $s \in (0,1)$, we first define the *Spectral fractional Laplacian* as

$$(-\Delta)^s u = \sum_{k=1}^{\infty} \lambda_k^s u_k \varphi_k$$

where $u_k = \int_\Omega u\varphi_k \, dx$, with $\{(\lambda_k, \varphi_k)\}_{k=1}^{\infty}$ denoting the eigenvalues and eigenfunctions of standard Laplacian with zero Dirichlet conditions, i.e., $-\Delta\varphi_k = \lambda_k\varphi_k$ in Ω and $\varphi_k = 0$ on $\partial\Omega$. The second definition is the so-called *Integral fractional Laplacian* given by

$$(-\Delta)^s u(x) = C_{N,s}\text{P.V.} \int_{\mathbb{R}^N} \frac{u(x) - u(y)}{|x-y|^{N+2s}} \, dy$$

where $C_{N,s}$ is a normalization constant and P.V. indicates the Cauchy principle value. It is clear from the second definition that fractional Laplacian is a nonlocal operator, unlike the standard Laplacian. See [2] and [10] for rigorous definitions of both these operators.

We discuss various novel numerical methods to solve fractional PDEs using reduced basis method [3, 13] via the so-called extension approach [11, 16, 14] or the Kato formula [12]. We also presented a novel spectral approach with almost linear complexity to solve fractional PDEs with integral fractional Laplacian [4].

We have paid special attention to optimal control problems with semilinear fractional PDEs as constraints. Here we also allow control constraints. In the

spectral case, we allow the control to be either in the interior or on the boundary [2]. In the integral case, the control is allowed to be in the interior [10] or in the exterior [6, 8]. We also present optimal control problems with fractional p-Laplacian (a quasilinear PDE) as constraints. The control here is given by the coefficient [9].

We conclude the talk by introducing a novel fractional operator where the fractional exponent is allowed to be spatially dependent instead of being a constant. Our approach is motivated by the extension approach. We allow the fractional exponent function to touch the extreme case of 0. We establish that, in this setting, we may not have density of smooth functions. We introduce novel function spaces and prove a trace theorem. Using this new operator as a regularizer in image denoising problems, we show that one can obtain almost perfect reconstructions which are significantly superior than TV based approaches [7].

References

[1] H. Antil and S. Bartels, *Spectral approximation of fractional PDEs in image processing and phase field modeling*, Computational Methods in Applied Mathematics **17**(4) (2017), 661–678.

[2] H. Antil, J. Pfefferer, and S. Rogovs, *Fractional operators with inhomogeneous boundary conditions: Analysis, control, and discretization*, Communications in Mathematical Sciences **16**(5) (2018) 1395–1426.

[3] H. Antil, Y. Chen, and A. Narayan, *Reduced basis methods for fractional Laplace equations via extension*, SIAM Journal on Scientific Computing **41**(6) (2019), A3552–A3575.

[4] H. Antil, D. Dondl, and L. Striet, *Approximation of Integral Fractional Laplacian and Fractional PDEs via* sinc-*Basis*, arXiv e-prints (Oct. 2020), arXiv:2010.06509.

[5] H. Antil, Z. Di, and R. Khatri, *Bilevel optimization, deep learning and fractional Laplacian regularizatin with applications in tomography*, Inverse Problems **36**(6) (2020), 064001-1–064001-22.

[6] H. Antil, R. Khatri, and M. Warma, *External optimal control of nonlocal PDEs*, Inverse Problems **35**(8) (2019), 084003-1–084003-35.

[7] H. Antil and C. N. Rautenberg, *Sobolev spaces with non-Muckenhoupt weights, fractional elliptic operators, and applications*, SIAM Journal on Mathematical Analysis **51**(3) (2019), 2479–2503.

[8] H. Antil, D. Verma, and M. Warma, *External optimal control of fractional parabolic PDEs*, ESAIM: Control, Optimisation and Calculus of Variations **26** (2020).

[9] H. Antil and M. Warma, *Optimal control of the coefficient for the regional fractional p-Laplace equation: approximation and convergence*, Mathematical Control and Related Fields **9**(1) (2019), 1–38.

[10] H. Antil and M. Warma, *Optimal control of fractional semilinear PDEs*, ESAIM: Control, Optimisation and Calculus of Variations **26** (2020).

[11] L. Caffarelli and L. Silvestre, *An extension problem related to the fractional Laplacian*, Communications in Partial Differential Equations **32**(7-9) (2007), 1245–1260.

[12] A. Bonito and J.E. Pasciak, *Numerical approximation of fractional powers of elliptic operators*, Mathematics of Computation **84**(295), 2083–2110.

[13] H. Dinh, and H. Antil, Y. Chen, E. Cherkaev, and A. Narayan, *Model reduction for fractional elliptic problems using Kato's formula*, arXiv e-prints (Apr. 2019), arXiv:1904.09332.

[14] R.H. Nochetto, E. Otárola, and A.J. Salgado, *A PDE Approach to Fractional Diffusion in General Domains: A Priori Error Analysis*, Foundations of Computational Mathematics **15**(3) (2015), 733–791.

[15] L.I. Rudin, S. Osher, and E. Fatemi, *Nonlinear total variation based noise removal algorithms*, Physica D: nonlinear phenomena **60** (1992), 259–268.
[16] P.R. Stinga and J.L. Torrea. *Extension problem and Harnack's inequality for some fractional operators*, Communications in Partial Differential Equations **35**(11) (2020), 2092–2122.
[17] C.J. Weiss, B.G. van Bloemen Waanders, and H. Antil, *Fractional operators applied to geophysical electromagnetics*, Geophysical Journal International **220**(2) (2020), 1242–1259.

Total curvature of curves in the C^1-closure of knot classes

Elisabeth Wacker

The Fary-Milnor theorem [1] gives a lower bound on the total curvature TC of a simple closed curve γ:

$$TC(\gamma) \geq 2\pi \cdot \mathrm{br}([\gamma]).$$

In this inequality, $\mathrm{br}([\gamma])$ denotes the bridge number of the knot class $[\gamma]$ that is the infimum of the number of minima which can be achieved in any one-dimensional projection of any curve in $[\gamma]$. Our goal is to transfer this bound to elements of the C^1-closure of the knot class in the following sense:

Theorem 1. *Let $(\gamma_k)_{k\in\mathbb{N}}$ be a sequence of simple closed curves in the same knot class, i.e., $[\gamma_k] = [\gamma_{k+1}]$ for all $k \in \mathbb{N}$, such that $\gamma_k \longrightarrow \gamma$ in C^1 as $k \to \infty$. Notice that the limit γ might contain self-intersections. The inequality*

$$TC(\gamma) \geq 2\pi \cdot br([\gamma_k])$$

holds for $\gamma \in W^{2,2}$ with only finitely many, isolated and transversal self-intersections, i.e., self-intersections with linearly independent tangents.

In its simplest form for bridge number 2 such a result was proven in using E. Denne's theorem on the existence of alternating quadrisecants [3] for every non-trivial knot. But this approach to prove a generalized Fary-Milnor theorem cannot be generalized to arbitrary bridge number. However, Theorem 1 could turn out to be quite useful to characterize elastic knots for more general knot classes than treated in [2].

We prove Theorem 1 using ambient isotopic deformations $\widehat{P}_k$ of γ_k which approximate the total curvature of γ such that

$$2\pi \cdot \mathrm{br}([\gamma_k]) \leq TC(\widehat{P}_k) \xrightarrow{k\to\infty} TC(\gamma).$$

For simplicity, we consider exactly one transversal self-intersection of finite multiplicity. The argumentation for all remaining self-intersections is analogous due to the isolation property. We start with defining polygons P_k inscribed in γ_k, i.e., polygons with vertices $\gamma_k(s)$ for a partition $S(k) \subset \mathbb{R}\backslash L\mathbb{Z}$ and $s \in S(k)$. W.l.o.g. we choose the partition $S(k)$ sufficiently fine to satisfy $[P_k] = [\gamma_k]$. We remark that P_k could contain more and more vertices with growing k, and this amount of vertices needs to be bounded in order to control the total curvature. We further transform P_k in two steps.

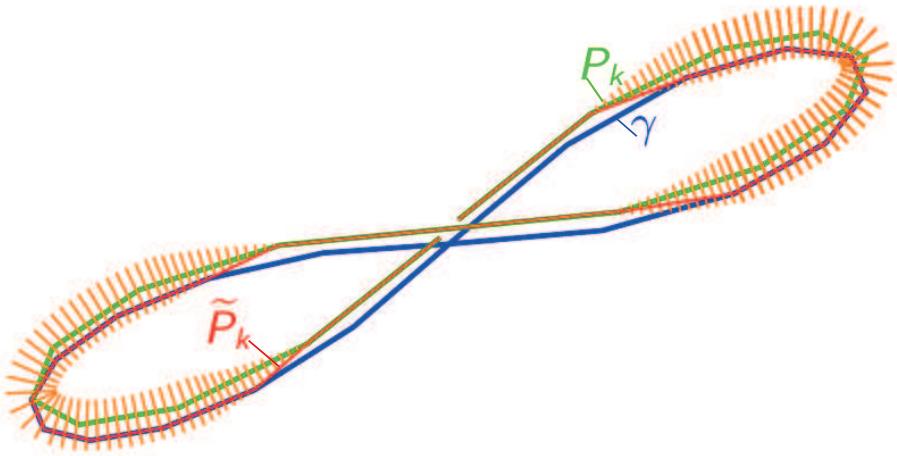

FIGURE 1. One self-intersection of multiplicity two: P_k is deformed to γ outside of the neighborhood $N(k)$ of the self-intersection of γ and thus yields $\widetilde{P}_k$.

Step 1: Outside a neighborhood $N(k)$ of the self-intersection, we deform P_k directly onto $\gamma \backslash N(k)$. For that, we define an explicit foliation of a compact neighborhood of P_k and γ consisting of disjoint, compact, convex and planar cross-sections such that both, P_k and γ, intersect each such cross-section transversely. This setting allows to apply [4, Theorem 1.2.4], which delivers the ambient isotopy between P_k and $\widetilde{P}_k$, where $\widetilde{P}_k$ equals P_k in $N(k)$ and γ outside of $N(k)$ except for some small transition zones between (see Figure 1).

Step 2: It remains to transform $\widetilde{P}_k$ inside $N(k)$. Let n be the multiplicity of the self-intersection of the limit curve γ and let the parameters $t_1, \dots t_n \in \mathbb{R} \backslash L\mathbb{Z}$ realize the self-intersection such that $\gamma(t_1) = \ldots = \gamma(t_n)$. We further define $\widetilde{P}_k^i, \widetilde{P}_k^j \subset \widetilde{P}_k \cap N(k)$ to be two fixed ropes of references (parts of the polygon $\widetilde{P}_k$ running through $N(k)$) for $1 \leq i < j \leq n$ and fix the planes

$$E_{ij} := \{x \in \mathbb{R}^3 | x \perp (\gamma'(t_i) \times \gamma'(t_j))\}.$$

Projecting $\widetilde{P}_k^i, \widetilde{P}_k^j$ for fixed i, j into the plane E_{ij} delivers pairwise unique self-intersections $\Pi_{E_{ij}}(\widetilde{P}_k^i) \cap \Pi_{E_{ij}}(\widetilde{P}_k^j)$. We fix all polygon edges of $\widetilde{P}_k^i$ which realize these self-intersections and construct open cones at the ends of the fixed edges with opening angles $\alpha(k) \xrightarrow{k\to\infty} 0$ and axes in the direction of $\pm\gamma'(t_i)$. We apply this construction for all P_k^i, $1 \leq i \leq n$ and intersect open cones facing each other to double cones (see Figure 2). Due to the transversality property, the so constructed cones are all disjoint and contain exactly one rope of reference running transverse through it. The cones might contain more and more vertices with growing k. However, we can now transform $\widetilde{P}_k$ between the apices to their direct connection

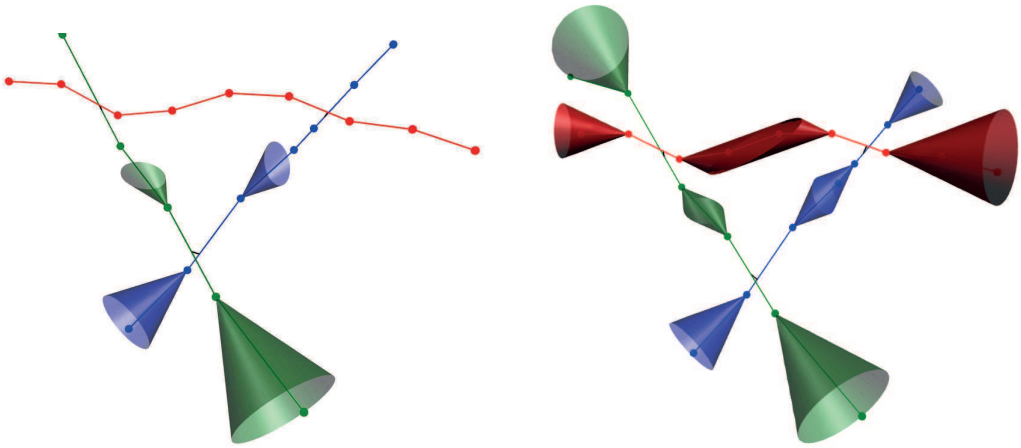

FIGURE 2. Example with self-intersection of multiplicity three: At the left, open cones are constructed at the ends of two edges whose projection in E_{ij} realizes a self-intersection $\Pi_{E_{ij}}(\widetilde{P}_k^i) \cap \Pi_{E_{ij}}(\widetilde{P}_k^j)$. At the right, all remaining open cones are added. The intersections of open cones facing each other constitute the double cones.

by ambient isotopies. We call the transformed polygon $\widehat{P}_k$ and then recalculate $TC(\widehat{P}_k) \xrightarrow{k\to\infty} TC(\gamma)$, which proves Theorem 1.

A follow-up question is how to prove the statement for limit curves with non-transversal self-intersections. The argumentation above does not apply because we can not guarantee that the constructed double cones are disjoint to yield well-defined ambient isotopies. Constructing other explicit ambient isotopies of γ_k approximating the total curvature of γ by an adapted procedure is work in progress.

REFERENCES

[1] J.W. Milnor, *On the total curvature of knots*, Annals of Mathematics. Second Series, **52**(2) (1950), 248–257.

[2] H. Gerlach, P. Reiter, and H. von der Mosel, *The elastic trefoil is the twice covered circle*, Archive for Rational Mechanics and Analysis **225** (2017), 89–139.

[3] E. Denne, *Alternating Quadrisecants of Knots*, arXiv e-prints (2005), arXiv:math/0510561.

[4] H. von der Mosel, *Lecture notes on a general construction of ambient isotopies (2020)*, in lecture series: Non-local curvature energies with applications to geometric knot theory, as yet unpublished.

Confined elastic rods

Pascal Weyer
(joint work with Sören Bartels)

Given a arc length parametrized curve $u : I = [0, L] \to \mathbf{R}^3$ with length L, its bending energy can be stated as

$$E_{\text{bend}}[u] = \frac{1}{2} \int_I |u''|^2 \mathrm{d}x.$$

This can be derived from three-dimensional plasticity theory by a rigorous dimension reduction [6]. Such curves then represent the centerline of an inextensible elastic rod embedded in $\mathbf{R}^3$. We focus on rods that are confined to a closed and convex domain D. Among them we seek for the least bent curve. This can be used to model DNA [5] or polymers [7] inside a cell. Therefore, we use a confinement energy functional that penalizes curves penetrating the space outside of D. Let $\varepsilon > 0$ and assume that D be defined as $D = \{y \in \mathbf{R}^3 : (y - m)^\top G_D (y - m) \leq 1\}$ for a symmetric and positive semi-definite matrix G_D and the center of mass m of D. Then the confinement penalty is defined as

$$\mathrm{CP}[u] = \frac{1}{2\varepsilon} \int_I \Big(\big((u - m)^\top G_D (u - m) \big)^{1/2} - 1 \Big)_+^2 \mathrm{d}x.$$

To minimize the sum of bending and confinement energy, we employ a gradient flow approach (cf. for instance [4]) that searches a solution of

$$(\partial_t u, v) = -\delta E_{\text{bend}}[u][v] - \delta \mathrm{CP}[u][v]$$

for all test functions v. To calculate the gradient flow numerically, we use a backwards time difference quotient to approximate $\partial_t u$. The curve u itself is projected onto a conforming finite-dimensional subspace of $H^2(I)$ and represented by piecewise cubic polynomials. The inextensibility of the curve ensures that the parametrization by arc length is maintained, i.e. that $|u'| = 1$ at all points in space and time. We impose the linearized version $[\partial_t u]' \cdot u'$ at the discrete nodes. The variation δE_{bend} is treated implicitly. The resulting scheme is unconditionally stable and was proposed for non-confined curves in [1]. The integrand of CP is split into a quadratic-convex and a concave part. The former is treated implicitly, the latter explicitly. This leads to unconditional stability also in the confined case. We can show that the pointwise penetration depth of u into $\mathbf{R}^3 \backslash D$ decreases for $\varepsilon \to 0$.

When numerically relaxing closed rods that are confined to a ball of radius R, interesting shapes arise as stationary points of the gradient flow. We find numerical evidence that these are in fact global minimizers of $E_{\text{bend}} + \mathrm{CP}$ for a fixed ratio $L/(2\pi R)$. The shapes can be classified into multiply covered circles and m-n-clews, cf. Figure 1. The former ones arise if $L/(2\pi R)$ is approximately an integer. The latter ones are fully described by two integers $m, n \geq 1$ with $\gcd(m, n) = 1$. We find two families, where either m or n is even, whereas the other one is odd. Assume that $L/(2\pi R) = p + \xi$ for an integer p and $\xi \in (0, 1)$. Then we find that

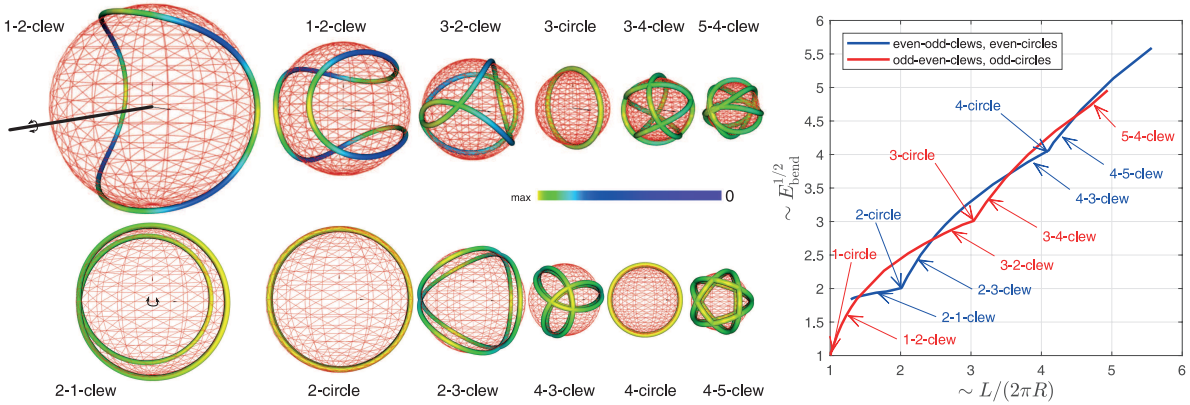

FIGURE 1. Left: Shapes of (numerical) elasticae for closed rods confined to balls. Colors indicate the pointwise curvature. Right: Energy scaling with the ratio $L/(2\pi R)$. Adapted from [2].

there is a threshold ξ_p such that both the p-$(p+1)$-clew and the $(p+1)$-p-clew have the same bending energy. If $\xi < \xi_p$, the p-$(p+1)$-clew is the stationary point with least bending energy found in our gradient flow experiments. For $\xi > \xi_p$, the numerically found elastica is the $(p+1)$-p-clew. Experiments that support this claim have been carried out up to $p = 4$. This finding is also illustrated in Figure 1. The 1-2-clew has also been observed for $L/(2\pi R)$ slightly larger than 1 in the setting of polymer rings [7].

So far, our numerical evidence furthermore indicates that we have found confined elasticae, that they all lie on the surface of the ball in the limit $\varepsilon \to 0$, and that the initial rod shape does not influence the final shape. It would be very insightful to find rigorous versions of these statements, possibly relating them to the findings of Brunnett and Crouch [3].

REFERENCES

[1] S. Bartels, *A simple scheme for the approximation of the elastic flow of inextensible curves*, IMA Jourbal of Numerical Analysis **33** (2013), 1115–1125.
[2] S. Bartels and P. Weyer, *A numerical scheme for confined, inextensible elastic rods*, in preparation.
[3] G. Brunnett and P. Crouch, *Elastic curves on the sphere*, Advances in Computational Mathematics **2** (1994), 23–40
[4] G. Dziuk, E. Kuwert, and R. Schätzle, *Evolution of elastic curves in* $\mathbf{R}^n$, SIAM Journal on Mathematical Analysis **33** (2002), 1228–1245.
[5] P. Furrer, R. Manning, and J. Maddocks, *DNA rings with multiple energy minima*, Biophysical Journal **79** (2000), 116–136.
[6] M. Mora and S. Müller, *Derivation of the nonlinear bending-torsion theory for inextensible rods by* Γ*-convergence*, Calculus of Variations and Partial Differential Equations **18** (2003), 287–305
[7] K. Ostermeir, K. Alim, and E. Frey, *Buckling of stiff polymer rings in weak spherical confinement*, Physical Review E **81** (2010), 061802-1–061802-8.

Simulation of self-avoiding plates

Christian Palus
(joint work with Sören Bartels, Frank Meyer)

In engineering and physics, a plate is defined as a (three-dimensional) structural element whose thickness is orders of magnitude smaller than its other dimensions. Thus, it seems natural to describe the bending behavior of a plate using a dimensionally reduced model. We consider a two-dimensional Kirchhoff model for bilayer plates, i. e. plates consisting of two thin layers with slightly different material properties, in which the energy corresponding to a deformation $y\colon \omega \to \mathbb{R}^3$ is given by

$$E_{\mathrm{bend}}[y] = \frac{1}{2}\int_\omega |II_y - \alpha \mathrm{I}_2|^2 \,\mathrm{d}x - \int_\omega f \cdot y \,\mathrm{d}x,$$

and the set of admissible deformations consists of mappings $y \in H^2(\omega;\mathbb{R}^3)$ that satisfy given clamped boundary conditions as well as the isometry constraint

$$[\nabla y]^\top \nabla y = \mathrm{I}_2$$

almost everywhere in ω. Here, the domain $\omega \subset \mathbb{R}^2$ is equivalent to the plate's midsurface in the reference configuration, $II_y(x)$ denotes the second fundamental form of the deformed surface, the parameter $\alpha \in \mathbb{R}$ describes the material mismatch between the two layers of the plate and $f\colon \omega \to \mathbb{R}^3$ is a given body force. This plate model can be rigorously derived from three dimensional elasticity in the limit of vanishing thickness [2,4,6].

Motivated by the findings in the context of self-avoiding inextensible curves [3], we augment the bending energy E_{bend} via addition of the tangent-point potential of the deformed surface [5,7], given for some $q \geq 2$ by

$$\mathrm{TP}[y] = \frac{2^{-q}}{q}\int_\omega \int_\omega \frac{1}{r^q(y(x), y(\widetilde{x}))}\mathrm{d}\widetilde{x}\mathrm{d}x,$$

where $r(y(x), y(\widetilde{x}))$ denotes the radius of the (unique) sphere which is tangent to the surface in $y(x)$ and intersects it in the point $y(\widetilde{x})$.

In order to numerically approximate minimizers of the resulting energy

$$E[y] = E_{\mathrm{bend}}[y] + \rho \mathrm{TP}[y],$$

with weighting parameter $\rho \geq 0$, we propose a practical method that is based on a discretization of the energy using DKT (discrete Kirchhof triangle) elements in space, cf. [1]. For the minimization of the discretized energy functional we choose a (discrete) H^2 scalar product $(\cdot,\cdot)_*$ as well as a pseudo time step size $\tau > 0$, and then employ the discrete gradient flow

$$\left(\tau^{-1}(y^k - y^{k-1}), w\right)_* = -E'_{\mathrm{bend}}[y^{k-\frac{1}{2}}; w] - \rho TP'[y^{k-1}; w]$$

which we restrict to appropriate tangent spaces arising from a linearization of the isometry constraint. The index $k - \frac{1}{2}$ represents a semi implicit treatment of the bending energy's variation, resulting in linear systems in every (pseudo-) time step. In the case $\rho = 0$ we establish Γ-convergence of the discrete energies towards

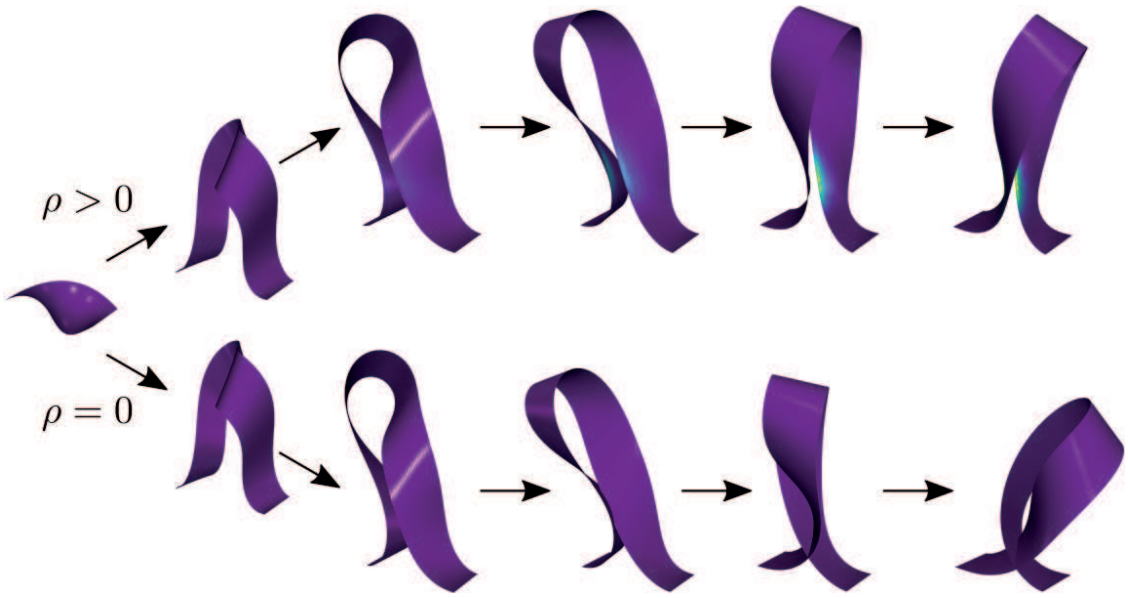

FIGURE 1. Approximating the minimal energy configuration of a twisted strip with compressive boundary conditions.

the continuous energy, as well as energy stability and a bound on the constraint error for the iterates in the discrete gradient flow under a mild condition on the step size τ. In the case $\rho > 0$ we present numerical experiments which indicate that self-intersections can be successfully prevented (Fig. 1). Drawbacks are long computation times on finer grids, and the fact that it is not clear a priori how the involved parameters τ, ρ, q need to be chosen to guarantee stability of the discrete gradient flow.

REFERENCES

[1] S. Bartels, *Approximation of large bending isometries with discrete Kirchhoff triangles*, SIAM Journal on Numerical Analysis **51** (2013), 516–525.

[2] S. Bartels, A. Bonito, and R. H. Nochetto, *Bilayer plates: model reduction, Γ-convergent finite element approximation, and discrete gradient flow*, Communications on Pure and Applied Mathematics **70** (2017), 547–589.

[3] S. Bartels, P. Reiter, and J. Riege, *A simple scheme for the approximation of self-avoiding inextensible curves*, IMA Journal of Numerical Analysis **38** (2018), 543–565.

[4] G. Friesecke, R. D. James, and S. Müller, *Rigorous derivation of nonlinear plate theory and geometric rigidity*, Comptes Rendus Mathematique **334**(2) (2002), 173–178.

[5] O. Gonzales and J. H. Maddocks, *Global curvature, thickness, and the ideal shapes of knots*, Proceedings of the National Academy of Sciences **96** (1999), 4769–4773.

[6] B. Schmidt, *Plate theory for stressed heterogeneous multilayers of finite bending energy*, Journal de Mathématiques Pures et Appliquées **88** (2007), 107–122.

[7] P. Strzelecki and H. von der Mosel, *Tangent-point repulsive potentials for a class of non-smooth m-dimensional sets in $\mathbb{R}^n$. Part I: Smoothing and self-avoidance effects*, Journal of Geometric Analysis, **23**(3) (2013), 1085–1139.

Ribbonlength of folded ribbon knots

Elizabeth Denne

Take a long thin strip of paper, tie a trefoil knot in it then gently tighten and flatten it. As can be seen in the figure below, the boundary of this "tight" trefoil knot is in the shape of a pentagon. L. Kauffman [7] introduced a mathematical model of such a *folded ribbon knot*. Kauffman viewed the ribbon as a set of rays parallel to a polygonal knot diagram with the folds acting as mirrors, and the over-under information appropriately preserved. An overview of the history of folded ribbon knots can be found in [3].

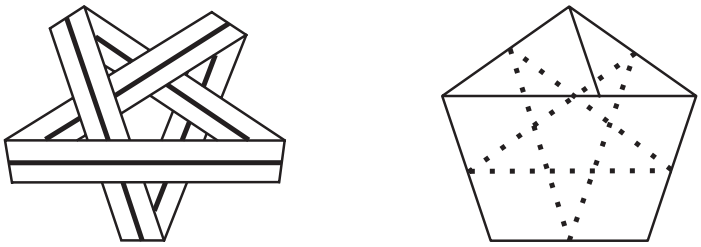

For a knot (or link) diagram K, we denote a folded ribbon knot as K_w, where w is the fixed width of the ribbon. We define the *folded ribbonlength* $\mathrm{Rib}(K_w)$ to be the length of K divided by the width of the ribbon. The *ribbonlength problem* asks to find the minimum folded ribbonlength needed to tie a folded ribbon knot for a particular knot or link type. There are a number of papers [1, 6, 7, 8, 9] which find upper bounds for folded ribbonlength of both specific knots and families of knots. For example, the pentagonal trefoil shown on the right in the figure above has folded ribbonlength $\mathrm{Rib}(K_w) \leq 5\cot(\pi/5) \leq 6.882$.

A separate, but equally interesting, open problem is to relate the ropelength of a knot K to its crossing number $\mathrm{Cr}(K)$. The *ribbonlength crossing number problem* asks us to find positive constants c_1, c_2, α, β such that

$$c_1 \cdot \mathrm{Cr}(K)^{\alpha} \leq \mathrm{Rib}(K) \leq c_2 \cdot \mathrm{Cr}(K)^{\beta}. \tag{1}$$

In 2017, Grace Tian [9] used grid diagrams to show that $\mathrm{Rib}(K) \leq 2\mathrm{Cr}(K)^2 + 6\mathrm{Cr}(K) + 4$. Thereby showing $\beta \leq 2$ for all knots and links. In 2020, we improved Tian's result (see [2]) to show that any non-split link type L with arc-index $\alpha(L)$ contains a folded ribbon link L_w such that

$$\mathrm{Rib}(L_w) \leq \begin{cases} 0.32\mathrm{Cr}(L)^2 + 1.28\mathrm{Cr}(L) + 0.23 & \text{when } \alpha(L) \text{ is even,} \\ 0.64\mathrm{Cr}(L)^2 + 2.55\mathrm{Cr}(L) + 2.03 & \text{when } \alpha(L) \text{ is odd.} \end{cases} \tag{2}$$

Also in [2], we proved that any knot or link type K contains a folded ribbon knot K_w such that

$$\mathrm{Rib}(K_w) \leq 72\mathrm{Cr}(K)^{3/2} + 32\mathrm{Cr}(K) + 12\sqrt{\mathrm{Cr}(K)} + 4. \tag{3}$$

We note that the larger expression in Equation 2 is smaller than Equation 3 when $\mathrm{Cr}(K) \leq 12,748$, and so both results are useful. However Equation 3 means that $\beta \leq 3/2$ for all knots and links in the ribbonlength crossing number problem.

Together with J.C Haden, T. Larsen and E. Meehan, we examined several infinite families of knots (see [4]). We used a variety of techniques to show these families of knots all have $\beta \leq 1$ in Equation 1. Namely,

- Any 2-bridge knot type K contains a folded ribbon knot K_w such that $\mathrm{Rib}(K_w) \leq 6\mathrm{Cr}(K) - 2$.
- Any $(2, p)$ torus knot type K contains a folded ribbon knot K_w such that $\mathrm{Rib}(K_w) \leq 2p = 2\mathrm{Cr}(K)$.
- Any pretzel knot type $K = P(p, q, r)$ contains a folded ribbon knot K_w such that $\mathrm{Rib}(K_w) \leq 2(|p| + |q| + |r|) + 2$. This result implies for certain families of pretzel knots and all twists knots that $\mathrm{Rib}(K_w) \leq 2\mathrm{Cr}(K) + 2$.

In addition, we found a completely new way of folding (p, q) torus knots. We proved (see [4]) that any (p, q) torus link type L (with $p, q \geq 2$) contains a folded ribbon link L_w such that $\mathrm{Rib}(L_w) \leq p+q$. This means that the trefoil knot can be constructed with a folded ribbonlength of 5! This is much smaller than previous known bounds ([7, 8, 9]). We used this bound to deduce the following.

Theorem 1 ([4])**.** *Suppose L is an infinite family (p, q) torus link types, where $p, q \geq 2$, and $p = aq + b$ for some $a, b \in \mathbb{Z}_{\geq 0}$. Then for each $q = 2, 3, 4, \ldots$, L contains a folded ribbon link L_w with*

$$\mathrm{Rib}(L_w) \leq 2\sqrt{2}\left(a + \frac{b}{2}\right)(\mathrm{Cr}(L))^{1/2}.$$

For example, for each $q = 2, 3, 4, \ldots$, the $(q + 1, q)$ torus link type contains a folded ribbon link L_w with $\mathrm{Rib}(L_w) \leq 3\sqrt{2}\mathrm{Cr}(L)^{1/2}$. Thus Theorem 1 gives evidence that $\alpha = 1/2$ in the ribbonlength crossing number problem.

There are many questions to be answered about folded ribbon knots.

(1) Minimizing folded ribbonlength of knot and link types. Just about all known examples give an upper bound on the minimum folded ribbonlength. Can we find lower bounds for folded ribbonlength?

(2) Relating folded ribbonlength to crossing number. Is it possible to find a different embedding of a knot such that $\mathrm{Rib}(K_w) \leq O(\mathrm{Cr}(K)^p)$ for some constant $1 \leq p < 3/2$? Alternatively, is there a family of knots and links for which folded ribbonlength has super-linear growth in crossing number?

(3) Folded ribbonlength and ribbon equivalence. A folded ribbon knot is a framed knot with ribbon linking number (given by the linking number of the knot diagram and one boundary component of the ribbon). Most of the previous work has ignored the framing of the ribbon when computing folded ribbonlength. We expect there to be a difference between folded ribbonlength bounds depending on the ribbon linking number. For example, in previous work [6], we showed that the ribbon linking number was different for two distinct $(5, 2)$ torus knots (given in [8]). We have also examined the folded ribbonlength of unknots with different ribbon linking numbers in [5, 8]. There is much to explore here.

References

[1] L. DeMaranville, textitConstruction of polygons by tying knots with ribbons, Master's Thesis, CSU Chico, Chico CA (1999).

[2] E. Denne, *Ribbonlength and crossing number for folded ribbon knots*, arXiv e-prints (Oct. 2020), arXiv:2010.03611.

[3] E. Denne, *Folded ribbon knots in the plane*, Chapter 88 of C. Adams, E. Flapan, A. Henrich, L. Kauffman, L. Ludwig, and S. Nelson (ed.), *Encylopedia of Knot Theory*, Taylor & Francis, 2020.

[4] E. Denne, J.C. Haden, T. Larsen, and E. Meehan, *Ribbonlength of families of folded ribbon knots*, arXiv e-prints (Oct. 2020), arXiv:2010.04188.

[5] E. Denne, and T. Larsen, *Minimizing ribbonlength of folded ribbon unknots*, preprint in preparation.

[6] E. Denne, M. Kamp, R. Terry, and X. Zhu, *Ribbonlength of folded ribbon unknots in the plane*, In: E. Flapan, A. Henrich, A. Kaestner, and S. Nelson (ed.), *Knots, Links, Spatial Graphs & Algebraic Invariants*, AMS Contemporary Mathematics, vol. 689, (2017) 37–51.

[7] L. H. Kauffman, *Minimal flat knotted ribbons*, In: J.A. Calvo, K. C. Millet, E. J. Rawdon, and A. Stasiak, *Physical and numerical models in knot theory*, Series on Knots and Everything vol. 36, World Scientific Publishing, Singapore (2005), 495–506.

[8] B. Kennedy, T. W. Mattman, R. Raya, and D. Tating, *Ribbonlength of torus knots*, Journal of Knot Theory and Its Ramifications **17**(1) (2008), 13–23.

[9] G. M. Tian, *Linear Upper Bound on the Ribbonlength of Torus Knots and Twist Knots*, MIT Summer Research Report (June 2017), `https://math.mit.edu/research/highschool/rsi/documents/2017Tian.pdf`, accessed August 6, 2020.

Injective nonlinear elasticity via surface penalty terms

Stefan Krömer

(joint work with Jan Valdman)

The parametrization of a deformed object representing an elastic body is the "deformation" map $y : \Omega \to \mathbb{R}^d$, linking the deformed body $\Omega \subset \mathbb{R}^d$ to its undeformed original shape, the "reference configuration". By contrast to geometric models for knots and other embedded manifolds, it encodes important information including local compression and stretching. In some elastic models, it is constrained to be "incompressible", i.e., locally volume preserving: $\det \nabla y = 1$. For $d = 1$, incompressible deformations are precisely local isometries, but the notions differ in higher dimensions. In general, however, an elastic material is usually at least slightly compressible, and in variational models of Nonlinear Elasticity governed by a local energy density $W(\nabla y(x))$ associated to y, the latter resists extreme local compressions in the sense that $W(F) \to +\infty$ as $\det F \to 0^+$. This implies a weak form of local injectivity for finite energy deformations, and global injectivity in an almost-everywhere sense can also be included in the model as a constraint, the Ciarlet-Nečas condition (CNC).

A numerical approach to compute elastic deformations satisfying (CNC) as critical points of an elastic energy was presented in [2]. As no numerically viable projection to (CNC) is known, global invertibilty is approximated by a penalty

term in the energy, which, similar to knot energies, acts repulsively once the deformation is close to self-contact. Reflecting the nonlocal character of global injectivity, it is a nonlocal functional, a double integral on Ω, which is computationally extremely expensive. A second drawback of [2] is that convergence (actually, Gamma-convergence) of the penalized energies to the constrained limit problem is only shown for models of non-simple materials whose elastic energy includes an additional regularizing term with higher order derivatives.

In our present work, we show how to obtain a more efficient penalty term which acts only on the surface, thereby reducing the effective dimension of the problem. In its simplest form, this surface penalty energy with parameters $\varepsilon, \beta > 0$, the latter fixed and the former the penalization parameter to be chosen as small as computationally feasible, is given by

$$E^{\partial\Omega}(y) := \frac{1}{\varepsilon^{\beta+d-1}} \int_{\partial\Omega} \int_{\partial\Omega} \left[|x - x'| - \frac{1}{\varepsilon} |y(x) - y(x')| \right]^+ d\mathcal{H}^{d-1}(x) d\mathcal{H}^{d-1}(x'),$$

where $[\cdot]^+$ denotes the positive part. It does not enforce added regularity of the deformation and therefore has at least a theoretical chance of (provably) working even for standard models of elasticity without higher order terms, where a Lavrientiev phenomenon can prevent the use of deformations with higher regularity.

As we will show for the regularized model where an energy bound ensures strictly orientation preserving deformations bounded in $C^{1,\alpha}$ or better, finiteness of $E^{\partial\Omega}(y)$ with ε small enough implies injectivity of $y|_{\partial\Omega}$ provided that $\beta > d-1$. Such deformations, as well as their possible weak limits in a Sobolev space associated to the elastic energy, are naturally *approximately invertible on the boundary* as defined in [1]. For topologically simple domains, the theory provided there in particular yields that (CNC) automatically holds – injectivity on the boundary transfers to the interior.

Whether or not similar results can be obtained for models without higher order terms is an open problem. While [1] does not need higher regularity, our analysis of the penalty term heavily uses that deformations are locally bi-Lipschitz, a property obtained from the interplay of the higher regularity of the deformations and the energy enforcing the integrability of $\det \nabla y^{-1}$ to a suitable power (using a result of Healey&.K., 2009). To what degree weaker bounds for the penalty term can be obtained from weaker assumptions remains to be seen. Another open problem is the convergence of forces (functional derivatives of the energy) stemming from the penalty term. Do they correctly predict forces caused by self-contact in the constrained limit problem?

In practice, the penalty term can be used for computations even without regularizing terms as well as for models of linear elasticty, as it is perfectly well defined in L^1 and just a compact perturbation of the elastic energy as long as ε is fixed. The crucial local bi-Lipschitz regularity of deformations needed for the limit analysis can in principle be checked a posteriori. Notice that outside of rather particular setups involving extreme external forces or boundary conditions, elastic materials usually do not have incentives to locally stretch or compress drastically.

References

[1] S. Krömer, *Global invertibility for orientation-preserving Sobolev maps via invertibility on or near the boundary*, Archive for Rational Mechanics and Analysis **238** (2020), 1113–1155.

[2] S. Krömer and J. Valdman, *Global injectivity in second-gradient nonlinear elasticity and its approximation with penalty terms*, Mathematics and Mechanics of Solids **24** (2019), 3644–3673.

On the analyticity of critical points for the generalized integral Menger curvature in the Hilbert case

Daniel Steenebrügge, Nicole Vorderobermeier

We prove the analyticity of smooth critical points $\gamma : \mathbb{R}/\mathbb{Z} \to \mathbb{R}^n$ for generalized integral Menger curvature energies [1, 2, 3]

$$\operatorname{intM}^{(p,2)}(\gamma) = \iiint\limits_{(\mathbb{R}/\mathbb{Z})^3} \frac{|(\gamma(y)-\gamma(x)) \wedge (\gamma(z)-\gamma(x))|^2 |\gamma'(x)||\gamma'(y)||\gamma'(z)| \,\mathrm{d}x\,\mathrm{d}y\,\mathrm{d}z}{|\gamma(y)-\gamma(x)|^p |\gamma(z)-\gamma(x)|^p |\gamma(z)-\gamma(y)|^p},$$

with $p = (\frac{7}{3}, \frac{8}{3})$, subject to a fixed length constraint. This implies, together with already well-known regularity results [3], that finite-energy, critical C^1-curves of generalized integral Menger curvature $\operatorname{intM}^{(p,2)}$ subject to a fixed length constraint are not only C^∞ but also analytic.

Our result serves as the last missing piece to complete the regularity theory of critical points for the subfamily of generalized integral Menger curvature energies stated above, which correspond to non-degenerate Euler-Lagrange operators. In case of the three-dimensional Euclidean space, analyticity of critical points implies that optimal representatives of knot types are analytic, fulfilling the expectation that knot energies like $\operatorname{intM}^{(p,2)}$ produce particularly nice embeddings as local minimizers.

Our approach is inspired by analyticity results on critical points for O'Hara's knot energies based on Cauchy's method of majorants [4, 5] and roughly works as follows: A curve $\gamma \in C^\infty(\mathbb{R}/\mathbb{Z}, \mathbb{R}^n)$ is analytic if and only if we have constants $C > 0$ and $r > 0$ such that for all $l \in \mathbb{N}_0$

$$\|\gamma^{(l)}\|_{L^\infty} \leq C \frac{l!}{r^l}.$$

Suppose we had a recursive estimate

$$\|\gamma^{(l+1)}\| \leq \Phi_l(\|\gamma\|, \ldots, \|\gamma^{(l)}\|)$$

and an analytic function $c : (-\varepsilon, \varepsilon) \to \mathbb{R}$ with

$$c^{(l+1)}(0) = \Phi_l(c(0), \ldots, c^{(l)}(0)) \text{ and } c(0) \geq \|\gamma\|.$$

Then, by induction,

$$0 \leq \|\gamma^{(l+1)}\| \leq \Phi_l(c(0), \ldots, c^{(l)}(0)) = c^{(l+1)}(0) \leq C \frac{(l+1)!}{r^{l+1}}$$

for all $l \in \mathbb{N}$ and so, γ is analytic.

In order to obtain this recursive estimate, we require a decomposition of the first variation given in [3] into a highest- and a lower-order part; $Q(\gamma)$ and $R(\gamma)$. For critical γ, these have pointwise equal absolute value. We show that

$$\|\gamma^{(l+3)}\|_{H^{m+3p-7}} \leq C\|\partial^l Q(\gamma)\|_{H^m}$$

and, with help of a fractional Leibniz rule, that

$$\|\partial^l R(\gamma)\|_{H^m} \leq C\Phi(\|\gamma'\|_{H^{m+\frac{3}{2}p-3}}, \dots, \|\gamma^{(l+2)}\|_{H^{m+\frac{3}{2}p-3}}).$$

Unlike in the cases inspiring our work, the resulting gap in orders of differentiability is smaller than 1, so the main new idea is an additional iteration in the recursive estimate of the derivatives to enable the induction presented above. This leads to an estimate of the form

$$\|\gamma^{(l+3)}\| \leq \Phi\big(\Phi(\|\gamma\|, \|\gamma'\|), \dots, \Phi(\|\gamma\|, \dots, \|\gamma^{(l+2)}\|)\big).$$

The corresponding analytic majorant can be found similarly to [4] but we have to use a second-order ODE to accommodate the nested terms.

We expect the method to be applicable to other self-repulsive energies as well as non-local differential equations in one or higher dimensions.

References

[1] O. Gonzalez and J. H. Maddocks, *Global curvature, thickness, and the ideal shapes of knots*, Proceedings of the National Academy of Sciences of the United States of America, **96**(9) (1999),4769–4773.

[2] P. Strzelecki, M. Szumańska, and H. von der Mosel, *Regularizing and self-avoidance effects of integral Menger curvature.* Annali della Scuola Normale Superiore di Pisa. Classe di Scienze. Serie V, **9**(1) (2010), 145–187.

[3] S. Blatt and Ph. Reiter, *Towards a regularity theory for integral Menger curvature*, Annales Academiae Scientiarum Fennicae Mathematica, **40**(1) (2015), 149–181.

[4] S. Blatt and N. Vorderobermeier, *On the analyticity of critical points of the Möbius energy*, Calculus of Variations and Partial Differential Equations, **58**(1) (2019) 16-1–16-28.

[5] N. Vorderobermeier. *On the regularity of critical points for O'Hara's knot energies: From smoothness to analyticity.* arXiv e-prints (Apr. 2019), arXiv:1904.13129.

Ideal knots: The trefoil, analysis and numerics to experiment

John Maddocks

Geometrical knot theory is an area of mathematics that has been growing in activity over the last few decades. It involves the study of specific shapes of knotted curves, rather than their topology, where the specific knot shape is fixed by some criterion, typically minimizing some form of knot energy. In this talk I will introduce some older work of both my collaborators and I, as well as others, on the specific case of ideal, or tightest, knot shapes. I will start by explaining the analytical difficulties, along with some associated theorems. Then I will describe some numerical results concentrating on the specific case of the ideal trefoil. And finally I will describe some very recent experimental results for the ideal trefoil obtained by the group of Pedro Reis at the EPFL.

Polyhedral discretizations of tangent-point energies

Henrik Schumacher

The *(generalized) tangent-point energy* of an n-dimensional, closed, embedded submanifold $\Sigma \subset \mathbb{R}^m$ is given by

$$\mathcal{E}_p^q(\Sigma) := \int_\Sigma \int_\Sigma \Phi(x,y)\,\mathrm{d}\mathcal{H}^n(y)\,\mathrm{d}\mathcal{H}^n(x), \quad \text{where} \quad \Phi(x,y) := \frac{|P(x)\,(y-x)|^q}{|y-x|^p}.$$

Here $P(x)$ denotes the orthoprojector onto $T_x\Sigma^\perp$, $\mathcal{H}^n$ denotes the n-dimensional Hausdorff measure and the exponents $q \geq 1$ and $p \geq 1$ are supposed to satisfy $2\,q - p + n > 0$. For $p = 2\,q$ the kernel reduces to the q-power of the inverse tangent-point radius: $\Phi(x,y) = r_{\mathrm{TP}}(x,y)^{-q}$.

It was shown in the case of $p = 2\,q$ [7] and in the case of $n = 1$, $q - p + 2\,n < 0$ [2] that these energies have beautiful self-avoidance properties. In particular, C^1-paths of finite energy in the space of embeddings cannot leave the isotopy class of the starting point. Moreover, embedded C^1-submanifolds have bounded tangent-point energy if and only if they are of fractional Sobolev-Slobodeckij class $W^{s,q}$ with $s = (p-n)/q$ [1]. All these properties make the tangent-point energies interesting as regularizers for various applications.

In order to make them amenable to numerical computations, these energies have to be discretized. Most standard pipelines for geometry processing work with simplicial meshes (e.g., polygonal lines for $n = 1$ and triangle meshes for $n = 2$). Although simplicial submanifolds have infinite tangent-point energy, a discrete analogue can readily be written down: Let $\mathcal{K} \subset \mathbb{R}^m$ be a simplicial mesh and denote by $\mathcal{T}$ the set of its n-simplices. Then the midpoint rule suggests the following *discrete tangent-point energy*:

$$\mathcal{E}_p^q(\mathcal{K}) := \sum_{S,\,T \in \mathcal{T},\ S \neq T} \frac{|P(S)\,(\bar{x}(T) - \bar{x}(S))|^q}{|\bar{x}(T) - \bar{x}(S)|^p}\,\mathcal{H}^n(S)\,\mathcal{H}^n(T).$$

Here $P(S)$ denotes the orthoprojector onto the normal space of the simplex S and $\bar{x}(S)$, $\bar{x}(T)$ are the barycenters of the simplices S and T.

Typically, the quadrature error of the midpoint rule can be controlled by the L^∞-norm of the second derivative of the integrand. However, even if Σ is smooth, the integrand $\Phi|_{\Sigma\times\Sigma}$ need not be continuous when $\dim(\Sigma) > 1$. This can be seen by recalling that the tangent-point radius $r_{\mathrm{TP}}(x,y)$ along C^2 curves approximates the curvature of the curve at x for $y \to x$: For $x \in \Sigma$ and $X \in T_x\Sigma$ we thus have

$$\Phi(x, \exp_x(X)) = |\mathrm{I\!I}_x(X,X)/|X|^2|^q\,|\exp_x(X) - x|^{2q-p} + o(|X|^{2q-p}) \quad \text{for } |X| \to 0,$$

where $\exp_x \colon T_x\Sigma \to \Sigma$ denotes the Riemannian exponential map and where $\mathrm{I\!I}_x \colon T_x\Sigma \times T_x\Sigma \to \mathbb{R}^m$ denotes the second fundamental form. For example, if we write $X = \varrho\,(e_1\cos(\varphi) + e_2\sin(\varphi))$ in polar coordinates with respect to unit principal curvature directions e_1, $e_2 \in T_x\Sigma$ with principal curvatures κ_1, κ_2, we obtain

$$\Phi(x, \exp_x(X)) = |\kappa_1\,\cos^2(\varphi) + \kappa_2\,\sin^2(\varphi)|^q\,\varrho^{2q-p} + o(\varrho^{2q-p}) \quad \text{for } \varrho \to 0. \tag{1}$$

Then for $n > 1$ and $p = 2\,q$, the limit of $\Phi(x, \exp_x(X))$ for $|X| \to 0$ does not exist. Thus, also the second derivatives of $\Phi|_{\Sigma\times\Sigma}$ have to blow up for $|x - y| \to 0$. So estimating the quadrature error is not as straight-forward and techniques similar to [5] and [4] have to be applied. The above analysis also tells us that some narrow band along the diagonal of $\Sigma \times \Sigma$ can be neglected. For example, if Σ is compact and has positive reach (so that $\mathrm{I\!I}$ is essentially bounded), then

$$\iint_{|y-x|\le\varrho} \Phi(x,y)\,\mathrm{d}\mathcal{H}^n(y)\,\mathrm{d}\mathcal{H}^n(y) = O(\varrho^{2q-p+n}) \quad \text{for } \varrho \to 0. \tag{2}$$

Hence we may focus on the complement of such a band. For simplicity and as a first step towards a rigorous error analysis, instead of inscribed simplices, we consider disjoint *patches* $S \subset \Sigma$ and $T \subset \Sigma$ satisfying $R(S,T) \coloneqq \inf\{|y - x| \mid x \in S,\, y \in T\} > 0$. We would like to compare their local energy contribution

$$\mathcal{E}_p^q(S,T) \coloneqq \int_S \int_T \Phi(x,y)\,\mathrm{d}\mathcal{H}^n(y)\,\mathrm{d}\mathcal{H}^n(x)$$

to their local contribution with respect to the midpoint rule

$$\mathcal{E}_{p,\mathrm{mid}}^q(S,T) \coloneqq \frac{|\bar{P}\,(\bar{y} - \bar{x})|^q}{|\bar{y} - \bar{x}|^p}\,\mathcal{H}^n(T)\,\mathcal{H}^n(S).$$

Here $\bar{P} \coloneqq \fint_S P(x)\,\mathrm{d}\mathcal{H}^n(x)$, $\bar{x} \coloneqq \fint_S x\,\mathrm{d}\mathcal{H}^n(x)$, and $\bar{y} \coloneqq \fint_T y\,\mathrm{d}\mathcal{H}^n(y)$ denote corresponding quantities averaged over S and T. We have the following result in which we measure the patch sizes by the *radii* $r(S) \coloneqq \sup\{|x - \bar{x}| \mid x \in S\}$ and $r(T) \coloneqq \sup\{|y - \bar{y}| \mid y \in T\}$:

Lemma 1. *Let $\Sigma \subset \mathbb{R}^m$ be a $C^{1,\beta}$-submanifold satisfying*

$$|P(x)\,(y - x)| \le K\,|y - x|^{1+\beta} \quad \text{and} \quad \|P(y) - P(x)\| \le K\,|y - x|^{\beta} \tag{3}$$

for some $K \ge 0$ and all x, $y \in \Sigma$. Suppose that the patches S, $T \subset \Sigma$ satisfy the separation condition *$0 < r(S)$, $r(T) \le h \le \theta\,R(S,T)$ for some $h > 0$ and $\theta > 0$. Then there is a $C > 0$ such that $\left|\mathcal{E}_p^q(S,T) - \mathcal{E}_{p,\mathrm{mid}}^q(S,T)\right|$ is bounded by*

$$C\,h^{2\beta} \int_S \int_T \left(\frac{|P(y)\,(y - x)|^{q-2}}{|y - x|^{p-2}} + \frac{\|P(y) - P(x)\|^{q-2}}{|y - x|^{p-q}} \right) \mathrm{d}\mathcal{H}^n(y)\,\mathrm{d}\mathcal{H}^n(x).$$

For a global approximation, one can decompose Σ into patches $\Sigma = \bigcup_{T\in\mathcal{P}} T$ with $r(T) \le h$ and approximate $\mathcal{E}_p^q(\Sigma)$ by the sum of all $\mathcal{E}_{p,\mathrm{mid}}^q(S,T)$, $(S,T) \in \mathcal{P} \times \mathcal{P}$ that satisfy $R(S,T) \ge \theta^{-1}h$. This way, only a band of width $\varrho \sim \theta^{-1}h$ is neglected. To illustrate the consequences, let us suppose again that Σ has finite reach and that $p = 2\,q$. Then β in Lemma 1 can be taken as $\beta = 1$. With (2) and (3) we obtain the following as error bound:

$$O(\varrho^n) + C''\,h^2 \iint_{|y-x|>\varrho} \frac{1}{|y - x|^2}\,\mathrm{d}\mathcal{H}^n(y)\,\mathrm{d}\mathcal{H}^n(x).$$

The latter integral is dominated by $\log(\mathrm{diam}(\Sigma)) - \log(\varrho)$ for $n = 1$ and by $\mathrm{diam}(\Sigma)^{n-1} - \varrho^{n-1}$ for $n > 1$. Thus, with $\varrho \sim h$ we obtain the following error rates: $O\big(h^1 + h^2\,(1 + |\log(h)|)\big) = O(h^1)$ for $n = 1$ and $O\big(h^n + h^2\,(1 + h^{n-1})\big) = O(h^2)$ for $n > 1$. Apparently, the consistency rate is better for $n > 1$ than for $n = 1$.

However, one has to keep in mind that polyhedral discretizations do not have direct access to patch averages: If $\tilde{S}$ is a simplex of radius h inscribed into a manifold Σ of positive reach and if $S \subset \Sigma$ is its metric projection onto Σ, then the orthoprojector of simplex S deviates from the average orthoprojector of patch S by $O(h)$. A rigorous analysis is yet to be performed, but these thoughts suggest that (i) one should expect a consistency rate of $O(h)$ for $\mathcal{E}^q_{2q}$ when Σ has positive reach, independent of the dimension n; and that (ii) higher order finite elements may achieve the optimal rate $O(h^2)$ for the midpoint rule, provided that $n > 1$. The numerical experiments carried out so far seem to verify these two conjectures. Moreover, in view of (1), it might be possible to improve the consistency of $\mathcal{E}^q_{2q}$ for curves of class $C^{2,1}$ to $O(h^2|\log(h)|)$ by adding a consistent discretization of $\iint_{|y-x|\leq\varrho} |\kappa(x)|^q \,\mathrm{d}\mathcal{H}^n(y)\,\mathrm{d}\mathcal{H}^n(x)$ (e.g., the one from [6]) instead of fully neglecting the diagonal.

Lemma 1 has a further practical consequence: Replacing h by $\theta^{-1}\,R(S,T)$, we can rewrite the error so that it becomes independent of the *absolute* patch size h:

$$C\,\theta^{2\beta} \int_S \int_T \left(\frac{|P(y)\,(y-x)|^{q-2}}{|y-x|^{p+2\beta-2}} + \frac{\|P(y)-P(x)\|^{q-2}}{|y-x|^{p+2\beta-q}} \right) \mathrm{d}\mathcal{H}^n(y)\,\mathrm{d}\mathcal{H}^n(x).$$

So instead of decomposing Σ into a collection of *small* patches, it suffices to decompose $\Sigma \times \Sigma$ into patch pairs $S \times T$ with small *relative* size, i.e., such that $\max(r(S), r(T)) \leq \theta\, R(S,T)$. This allows one to group many nearby simplices together into a single patch. Then for two such patches, instead of computing all the pairwise interactions, one just has to compute the single interaction between the patches' averages. Algorithms like the *Barnes-Hut method* and the *fast multipole method* exploit this systematically to reduce the effort for computing the energy $\mathcal{E}^q_p(\mathcal{K})$ of a simplicial surface $\mathcal{K}$ with N faces from $O(N^2)$ to $O(N\log(N))$. These techniques have already been applied to the tangent-point energy of curves [3]; a transfer to the tangent-point energy of surfaces is under current development by the same authors.

Acknowledgements. This work is supported by the DFG project 282535003: *Geometric curvature functionals: energy landscape and discrete methods.*

References

[1] S. Blatt, *The energy spaces of the tangent point energies*, Journal of Topology and Analysis **5**(3) (2013), 261–270.

[2] S. Blatt and P. Reiter, *Regularity theory for tangent-point energies: the non-degenerate sub-critical case*, Advanced Calculus of Variations **8**(2) (2015), 93–116.

[3] Chr. Yu, H. Schumacher, and K. Crane, *Repulsive curves*, arXiv e-prints (Apr. 2020), arXiv:2006.07859, to appear in ACM Transactions on Graphics.

[4] A. M. Lagemann, *Discrete tangent-point energies on biarc-curves and Γ-convergence*, master's thesis, RWTH Aachen University, (2019).

[5] S. Scholtes, *Discrete Möbius energy*, Journal of Knot Theory and Its Ramifications **23**(9) (2014), 1450045-1–1450045-16.

[6] S. Scholtes, H. Schumacher, and M. Wardetzky, *Variational convergence of discrete elasticae*, IMA Journal of Numerical Analysis, **12** (2020).
[7] P. Strzelecki and H. von der Mosel, *Tangent-point repulsive potentials for a class of non-smooth m-dimensional sets in $\mathbb{R}^n$. Part I: Smoothing and self-avoidance effects*, Journal of Geometric Analysis, **23**(3) (2013), 1085–1139.

Reporter: Henrik Schumacher

Participants

Prof. Dr. Harbir Antil
Department of Mathematical Sciences
George Mason University
4400 University Drive, MS: 3F2
Fairfax VA 22030-4444
UNITED STATES

Prof. Dr. Lothar Banz
Fachbereich Mathematik
Universität Salzburg
Hellbrunnerstr. 34
5020 Salzburg 5020
AUSTRIA

Prof. Dr. Sören Bartels
Abteilung für Angewandte Mathematik
Universität Freiburg
Hermann-Herder-Strasse 10
79104 Freiburg i. Br.
GERMANY

Prof. Dr. Simon Blatt
Fachbereich Mathematik
Universität Salzburg
Hellbrunnerstrasse 34
5020 Salzburg
AUSTRIA

Prof. Dr. Elizabeth Denne
Department of Mathematics
Washington and Lee University
Lexington, VA 24450
UNITED STATES

Priv.-Doz. Dr. Stefan Krömer
UTIA
Czech Academy of Sciences
Pod vodarenskou vezi 4
18200 Praha
CZECH REPUBLIC

Anna Lagemann
Institut für Mathematik
RWTH Aachen University
Templergraben 55
52062 Aachen
GERMANY

Prof. John H. Maddocks
Mathématiques Département
École Polytechnique Fédérale de Lausanne
Station 8
1015 Lausanne
SWITZERLAND

Christian Palus
Abteilung für Angewandte Mathematik
Universität Freiburg
Hermann-Herder-Strasse 10
79104 Freiburg i. Br.
GERMANY

Prof. Dr. Philipp Reiter
Fakultät für Mathematik
Technische Universität Chemnitz
09107 Chemnitz
GERMANY

Prof. Dr. Armin Schikorra
Department of Mathematics
University of Pittsburgh
301 Thackery Hall
PA Pittsburgh 15260
UNITED STATES

Dr. Henrik Schumacher
Institut für Mathematik
RWTH Aachen University
Templergraben 55
52062 Aachen
GERMANY

Daniel Steenebrügge
Institut für Mathematik
RWTH Aachen University
Templergraben 55
52062 Aachen
GERMANY

Prof. Dr. Pawel Strzelecki
Instytut Matematyki
Uniwersytet Warszawski
ul. Banacha 2
02-097 Warszawa
POLAND

Prof. Dr. Heiko von der Mosel
Institut für Mathematik
RWTH Aachen University
Templergraben 55
52062 Aachen
GERMANY

Nicole Vorderobermeier
Fachbereich Mathematik
Universität Salzburg
Hellbrunnerstrasse 34
5020 Salzburg
AUSTRIA

Elisabeth Wacker
Institut für Mathematik
RWTH Aachen
Templergraben 55
52062 Aachen
GERMANY

Pascal Weyer
Mathematisches Institut
Universität Freiburg
Ernst-Zermelo-Str. 1
79104 Freiburg i. Br.
GERMANY